Time- and frequency-gated spontaneous emission as a tool for studying vibrational dynamics in the excited state

M. F. Gelin,[1] A. V. Pisliakov,[2] and W. Domcke[2]
[1]*Institute of Molecular and Atomic Physics, National Academy of Sciences of Belarus, Skaryna Avenue, 70, Minsk 220072, Belarus*
[2]*Institute of Physical and Theoretical Chemistry, Technical University of Munich, 85747 Garching, Germany*
(Received 25 October 2001; published 17 June 2002)

The theory of time- and frequency-gated (TFG) spontaneous emission (SE) spectra is elaborated. The present formulation generalizes previous derivations, clarifies the interrelations between different existing expressions, and establishes the validity of certain commonly assumed approximations. We obtain various explicit expressions for TFG SE spectra, which are suitable for performing actual calculations for nontrivial systems and which allow us to establish generic (that is, model-independent) properties of TFG spectra. The doorway-window picture of temporally and spectrally resolved spectra is further developed. It is shown that, to the leading order in the pump and probe pulses, the TFG SE signal is equivalent to the stimulated-emission contribution to the integral pump-probe spectrum in the case of nonoverlapping pulses. The theory is illustrated for the example of an electronic two-level system with a single Condon-active harmonic vibrational mode that is coupled to a thermal bath. The effect of imperfect time and frequency resolution is studied. It is pointed out that the TFG SE spectrum carries information not only on the strength of the system-bath coupling, but also on the relative magnitude of the bath correlation time.

DOI: 10.1103/PhysRevA.65.062507 PACS number(s): 33.70.Jg, 78.47.+p

I. INTRODUCTION

Spectroscopic measurements are conventionally performed either in the time or in the frequency domain. The two kinds of experiments can, however, be successfully combined, thereby allowing us to follow the time evolution of spectra [1–3]. Provided that sufficient temporal and spectral resolution has been achieved, these techniques make it possible to monitor the relaxation to equilibrium of a material system that has been excited by a short laser pulse. When interpreting such experiments, a fundamental question arises: how can one extract quantitative information on the dynamics of a material system from the measured signals?

The present paper is devoted to the consideration of the time- and frequency-gated (TFG) spontaneous emission (SE). We restrict ourselves to the simplest (but important) case when the excitation and emission processes are well separated temporally. Under these conditions, the SE consists primarily of the fluorescence component; the Raman contribution can be neglected due to fast optical dephasing [1–3].

The first experimental observation of coherent wave-packet dynamics via the TFG SE technique was reported in Ref. [4] for the sodium dimer (see also Refs. [5–7]). Later on, coherent effects in TFG SE responses have been measured for diverse systems, ranging from diatomic molecules to polyatomic donor-acceptor complexes [1–10]. By monitoring the SE, one gets the opportunity to keep track of vibrational wave-packet dynamics in the electronically excited state as well as decay of the excited state. Therefore the TFG SE spectroscopy is a promising tool for the elucidation of ultrafast excited-state relaxation in systems with pronounced nonadiabatic couplings [2,11–17].

There exist two major approaches to the description of the TFG SE. In the first approach, the TFG SE spectrum is defined as the rate of emission of photons of a certain frequency within a definite time interval. The influence of the measuring device is not taken into account in this formulation [1,12,14–22]. Starting from this definition, one obtains an ideal (bare) TFG SE spectrum, which is not guaranteed to be positive, however. For instance, for certain parameters of the Brownian oscillator model, the spectrum can attain negative values [1,3]. Moreover, the time and frequency resolution of this ideal spectrum are not limited by the fundamental time-frequency uncertainty principle. This underlines the necessity to develop a more comprehensive theory, in which both a spectrometer and a time-gating device enter the description from the outset.

This is the characteristic feature of the second group of approaches, in which the TFG SE is taken to be proportional to the integrated intensity of the total emitted field that has passed through a spectrometer and a temporal gating device [23,24]. Following the guidelines developed in Ref. [23], the TFG SE has been investigated by a number of authors [2,5–7,13,25,26]. The explicit consideration of the TFG process adds, however, additional complexity to the problem, and it is therefore not surprising that the papers [5–7,25,26] deal with one-dimensional dissipation-free systems, which allows the description of the material dynamics in terms of the eigenvalues and eigenfunctions of the Hamiltonian. Cina and coworkers have formulated a theory that is intermediate between the two approaches [3,27,28]. These authors have investigated the influence of the time gate on the intensity [3,27] and anisotropy [28] of the SE, while the frequency resolution was tacitly assumed to be perfect. Mukamel and coworkers have developed a general description, which ensures a correct inclusion of the TFG process for any material system under study [29–31]. The passage to an ideal gate also has been briefly discussed by these authors.

The formulations developed in Refs. [29–31] provide deep insight into the problem of the TFG SE. However, their implementation for the calculation of the TFG SE is difficult

for complex material systems, due to the necessity to perform numerous time integrations and Fourier transforms involving multitime response functions. Moreover, several other questions deserve further clarification and investigation. The papers [29–31], as well as the pivotal paper [23], are based on the assumption that the emitted field is proportional to the transition dipole moment. This is a good approximation for spectrally narrow bands, but, in a more general context, it may be necessary to go beyond this approximation [13]. In addition, the excitation pulse is treated perturbatively in Refs. [29–31], which may not be appropriate for typical experiments that employ a short, but not necessarily, weak laser pulse.

Explicit calculations of the TFG SE for dissipative systems have so far been performed only for the classical overdamped Brownian oscillator [29,30] and, very recently, for molecular aggregates within the Redfield theory [32,33]. Important questions concerning the manifestation of different regimes of the bath-induced vibrational relaxation in the TFG SE have not yet been addressed. An important issue is to clearly separate the contributions due to the material system dynamics from those of the measuring device in the TFG SE signal. The two groups of approaches to the TFG SE, [1,12,14–21] and [2,5–7,13,25,26,29–33], have so far been developed separately from each other, so that their interrelationship is not obvious. It is also of importance to establish more rigorously the interconnection between the TFG SE signal and other spectroscopic signals, in particular transient absorption pump-probe signals.

This state of affairs indicates the necessity to cast the TFG spectrum in a form that is computationally convenient, but not limited to a particular or simple material-system dynamics. To achieve this goal, it seams promising to further develop the doorway-window (DW) picture of the TFG SE. This has partially been done already in papers [3,27] (for perfect spectral filters) and in Refs. [29–33] (for ''bare'' spectra, which are connected with ''real'' TFG SE spectra through the convolution with the joint time-frequency gate function). The aim of the present paper is to directly develop the DW description for ''real'' TFG SE spectra. This formulation reduces the computational effort considerably, since some of the integrals can be performed analytically. Concomitantly, this formulation allows us to make the interrelations between the approaches mentioned above more transparent and to obtain various forms of the expressions that can be useful in actual calculations. It is hoped that the proposed theory will simplify the computation of the TFG SE for nontrivial multidimensional systems, in particular, those exhibiting pronounced nonadiabatic couplings and therefore ultrafast decay dynamics.

The paper is organized as follows. The definitions of the TFG SE signals are introduced in Sec. II. Several generic properties of the TFG SE are established in Sec. III. This analysis provides insight into the information content of TFG SE spectra. In Sec. IV the DW picture of TFG SE is developed, in the limit when excitation and gating pulses do not overlap. If, moreover, the pump pulse can be regarded as truly instantaneous, the DW description is generalized beyond this limit, which allows the study of the influence of transient terms on the TFG SE. Section V contains the results of calculations of TFG spectra for the Drude oscillator model. The analysis focusses both on the strength of the system-bath coupling, as well as on the effect of the bath relaxation time. The latter issue can be of importance for the interpretation of ultrafast time-domain experiments (see, e.g., Ref. [34] and references cited therein). By considering different regimes of temporal gating and frequency filtering, we show to what extent the measurable signals reflect the intrinsic wave packet motion. Concluding remarks are contained in Sec. VI.

For notational convenience, we use units in which $\hbar=1$.

II. DEFINITION OF TFG SPECTRA

The total intensity of the temporally gated and spectrally filtered field at the position $\vec{r}$ in the far-field region is given by the general expression [23]

$$S_{st}(t_0,\omega_0)\sim\int_{-\infty}^{\infty}dt\int_{-\infty}^{\infty}dt'\int_{-\infty}^{\infty}dt''E_t(t';t_0)E_t^*(t'';t_0)\times F_s(t-t',\omega_0)F_s^*(t-t'',\omega_0)\times\langle E(\vec{r},t')E(\vec{r},t'')^*\rangle. \quad (1)$$

Here $E_t(t;t_0)$ is the time-gate function that is strongly peaked near the gating time $t\sim t_0$, the function $F(t-t',\omega_0)$ is responsible for the spectral filtering near the central frequency ω_0, and $\langle E(\vec{r},t')E(\vec{r},t'')^*\rangle$ is the correlation function (CF) of the emitted field. It is clear from this definition that the TFG SE spectrum is always positive, in contrast to its bare counterpart [1,3]. We shall further use the standard approximations [5,6,13,23–26,29–31]

$$E_t(t;t_0)=\exp\{-[\Gamma(t-t_0)]^2\} \quad (2)$$

or

$$E_t(t;t_0)=\exp(-\Gamma|t-t_0|) \quad (3)$$

for the time-gate function and

$$F_s(t,\omega_0)=\vartheta(t)\frac{\gamma}{2}\exp\{-(\gamma+i\omega_0)t\},$$

$$F_s(\omega,\omega_0)=\frac{\gamma^2}{\gamma^2+(\omega_0-\omega)^2} \quad (4)$$

for the frequency filter (which is a good approximation for the Fabry-Perot filter [23]). The constants Γ and γ determine the widths of the corresponding filters, $\vartheta(t)$ is the Heaviside step function that ensures causality, and Fourier transforms are denoted as

$$f(\omega)\equiv\int_{-\infty}^{\infty}dt\,f(t)e^{i\omega t}\quad\forall\, f(t).$$

Following Ref. [23], we normalize the TFG spectrum according to the condition that the total energy passed through the TFG filter is equal to the emitted energy, namely,

$$C\int_{-\infty}^{\infty}\frac{dt_0\,d\omega_0}{2\pi}S_{st}(t_0,\omega_0)=\int_{-\infty}^{\infty}dt\langle|E(\vec{r},t)|^2\rangle. \quad (5)$$

The normalization constant C is readily obtainable for the TFG functions (2)–(4). One gets

$$C=8\xi\Gamma/\gamma, \quad (6)$$

with $\xi=\sqrt{2/\pi}$ for Gaussian (2) and $\xi=1$ for the exponential (3) time gate.

It is straightforward to demonstrate that the light emitted by a collection of independent dipoles in the far-field region is proportional to the second derivative of the optically induced polarization [13,30,35]

$$\vec{E}(\vec{r},t)=-\frac{2\pi}{c^2r}\frac{d^2}{dt^2}\vec{P}(\vec{r},t-\tau_r). \quad (7)$$

Here c is the speed of light, and $\tau_r\equiv r/c$ is the retardation time. Integrating the CF of the emitted light over a small solid angle on the sphere of radius r, one arrives at the expression

$$\langle E(\vec{r},t')E(\vec{r},t'')^*\rangle\sim\frac{d^2}{dt'^2}\frac{d^2}{dt''^2}\langle P(t'-\tau_r)P(t''-\tau_r)\rangle. \quad (8)$$

In order to derive the TFG SE signal from this definition, it is a standard practice in the literature (a) to neglect by the retardation effects ($\tau_r\equiv 0$) and (b) to invoke the slowly varying envelope approximation, i.e., $\partial_t^2\vec{P}(t)\approx-\omega^2\vec{P}(t)$, where ω is the carrier frequency. That is tantamount to the assumption

$$\langle E(\vec{r},t')E(\vec{r},t'')^*\rangle\sim\langle P(t')P(t'')\rangle. \quad (9)$$

Here we would like to analyze the above assumptions in some detail.

(a) Starting from the definition (1), it is elementary to demonstrate that one obtains the signal $S_{st}(t_0-\tau_r,\omega_0)$ from the retarded CF $\langle P(t'-\tau_r)P(t''-\tau_r)\rangle$, if the unretarded CF $\langle P(t')P(t'')\rangle$ gives the signal $S_{st}(t_0,\omega_0)$. [In the derivation of this result, it has been assumed that $E_t(t;t_0)=E_t(t_0-t)$, which is a natural approximation for a time gate.] The retardation thus merely gives rise to a shifted time origin of the TFG spectrum. Keeping this in mind, we put $\tau_r\equiv 0$ in all subsequent calculations. It should be pointed out, however, that for $r=1$ cm, for example, one gets $\tau_r=100$ ps, so that it is necessary to decide in a particular ultrafast experiment if the consideration of retardation effects is important or not.

(b) By expressing the frequency-gate functions through their Fourier transforms and inserting the corresponding formulas into Eq. (1), one gets

$$S_{st}(t_0,\omega_0)=\int_{-\infty}^{\infty}d\omega_1|F_s(\omega_1,\omega_0)|^2\,S_t(t_0,\omega_1), \quad (10)$$

where

$$S_t(t_0,\omega_1)\sim\int_{-\infty}^{\infty}dt'\int_{-\infty}^{\infty}dt''\exp[-i\omega_1(t'-t'')]E_t(t';t_0)\times E_t^*(t'';t_0)\frac{d^2}{dt'^2}\frac{d^2}{dt''^2}\langle P(t')P(t'')\rangle \quad (11)$$

is the TFG spectrum obtained with ideal spectral resolution [$|F_s(\omega,\omega_0)|^2=\delta(\omega-\omega_0)$]. The spectral filtering is seen to be independent of the time gating and material system dynamics, so that its effect on the TFG SE can always be removed by deconvolution [29–31]. Proceeding in the spirit of papers [29–31], one can use Eq. (11) to develop generalized Wigner spectrograms for the description of the TFG SE (see Appendix). For the purpose of the further presentation, we prefer to stay in the time domain. Integrating Eq. (11) by parts, one transfers the action of the time derivatives from the polarization CF to the time-gate functions, so that

$$S_t(t_0,\omega_0)\sim\int_{-\infty}^{\infty}dt\int_{-\infty}^{\infty}dt'\,\overline{E}_t(t;t_0)\overline{E}_t^*(t';t_0)\times\exp[-i\omega_0(t-t')]\langle P(t)P(t')\rangle, \quad (12)$$

where

$$\overline{E}_t(t;t_0)=\left(\frac{d^2}{dt^2}-2i\omega_0\frac{d}{dt}-\omega_0^2\right)E_t(t;t_0). \quad (13)$$

The explicit inclusion of the time derivatives in the definition of the TFG SE results in a redetermination of the time-gate functions. For instance, starting from Eq. (2), one gets

$$\overline{E}_t(t;t_0)=\{[\Gamma^2(t-t_0)+i\omega_0]^2-\Gamma^2\}E_t(t;t_0). \quad (14)$$

Formally speaking, these generalized gate functions become complex and frequency dependent, but the product $\overline{E}_t(t;t_0)\overline{E}_t^*(t';t_0)$ is of course real. The inspection of the above equations allows one to estimate a criterion for the validity of Eq. (9). In an experiment with ultrafast time resolution, one normally has $\Gamma\gg\gamma$ (a good filter), Γ being the inverse of the gating-pulse duration. If the material system under study possesses a narrow spectrum in the vicinity of the relatively well defined frequency $\omega_{eg}\gg\Gamma$ of an electronic transition, then $\overline{E}_t(t;t_0)\approx-\omega_0^2E_t(t;t_0)$. When the system under study exhibits a broad or multipeaked spectrum, one should use the more general expressions (12) and (13). Keeping in mind the above restrictions, we shall use formula (9) as the basic equation for the analysis of the TFG SE.

III. GENERAL PROPERTIES OF TFG SPECTRA

Adopting the standard Fabry-Perot-like form (4) of the frequency filter, one can immediately perform the integration over t in Eq. (1) analytically. This yields

$$S_{st}(t_0,\omega_0)=C'\int_{-\infty}^{\infty}dt\int_{-\infty}^{t}dt'\,E_t(t;t_0)E_t^*(t';t_0)\times[\exp\{-(\gamma+i\omega_0)(t-t')\}\times\langle E(\vec{r},t)E(\vec{r},t')^*\rangle+\text{c.c.}]. \quad (15)$$

Here a new normalization constant, $C'=C\gamma/4$, has been introduced. According to Eq. (6), it is independent of the frequency filter resolution γ. We shall further accept the assumption (9), so that

$$S_{st}(t_0,\omega_0)\sim\mathrm{Re}\int_{-\infty}^{\infty}dt\int_{-\infty}^{t}dt'E_t(t;t_0)E_t^*(t';t_0)\times\exp\{-(\gamma+i\omega_0)(t-t')\}\langle P(t)P(t')\rangle. \quad (16)$$

By calculating $P(t)$ to first order in the pump, employing the rotating-wave approximation [36], retaining only sequential contributions (excitation precedes gating), and performing some standard manipulations (see, e.g., Refs. [1,29–31]), one arrives at the result

$$S_{st}(t_0,\omega_0)\sim\mathrm{Re}\int_{-\infty}^{\infty}dt\int_{0}^{\infty}dt_3\int_{0}^{\infty}dt_2\int_{0}^{\infty}dt_1E_t(t-t_0)\times E_t(t-t_3-t_0)E_L(t-t_3-t_2)\times E_L(t-t_3-t_2-t_1)e^{-(\gamma-i\omega_0)t_3}\times\{R_1(t_3,t_2,t_1)e^{i\omega_Lt_1}+R_2(t_3,t_2,t_1)e^{-i\omega_Lt_1}\}. \quad (17)$$

Here the frequency ω_L and the envelope $E_L(t)$ characterize the excitation pulse, and $R_i(t_3,t_2,t_1)$, $i=1,2$, are the third-order nonlinear response functions [1]. Clearly, if there is no time gating ($\Gamma=0,E_t=1$), then the TFG spectrum reduces to the frequency-domain fluorescence spectrum [see Eq. (9.10b) in Ref. [1]]. On the other hand, by comparing Eq. (17) with Eq. (11.8) in Ref. [1], one immediately realizes that the TFG SE is nothing else than the excited-state (stimulated-emission) contribution to the integrated pump-probe spectrum for nonoverlapping pulses. The filter thus defines an effective carrier frequency ω_0 of the probe, and the temporal gate function represents the probe envelope centered at t_0. The only difference stems from the imperfection of the frequency filter γ, which controls the spectral resolution of the TFG SE. For an ideal filter ($\gamma=0$) the analogy is complete, and one recovers the equations derived in Refs. [3,27].

A close similarity between the TFG SE and pump-probe spectra has repeatedly been emphasized in the literature [1–3,14,15,22]. It should be noted, however, that the equivalence between the TFG SE signal and stimulated-emission contribution to the sequential integral pump-probe signal holds only in the leading (second) order in the pump and probe pulses. In this case also the ''bare'' TFG SE spectrum coincides with the stimulated-emission contribution to the dispersed pump-probe spectrum [14,15]. It is of importance that both stimulated emission (from the electronically excited state) and stimulated Raman (from the ground state) processes contribute to the overall pump-probe signal, even in the case of sequential, nonoverlapping pump and probe pulses. On the other hand, if the excitation and gate pulses do not overlap, the SE consists solely of the fluorescence (excited state) component. As a consequence, one cannot experimentally separate the ground and excited state contribution to the pump-probe signal. The SE signal from the excited state is, however, background free. So, in general, the TFG SE is not simply related to the pump-probe signal.

For our further purposes it is convenient to develop the DW representation of the TFG spectrum. To simplify the presentation, we confine ourselves to the case of a single optical transition between electronic states. We write the Hamiltonian as

$$H=\begin{pmatrix}H_g & 0\\ 0 & H_e\end{pmatrix}. \quad (18)$$

Here H_α are the total (system plus bath) vibrational Hamiltonians in the ground state ($\alpha=g$) and the excited electronic state ($\alpha=e$). While this form of the Hamiltonian excludes intramolecular nonadiabatic coupling of the excited electronic state with the ground state, it should be stressed that H_e may represent several nonadiabatically coupled electronic states. The ensuing formulation includes, in particular, the case of an optically bright excited state that is intramolecularly coupled to one or several optically dark states. Although the form (18) of the molecular Hamiltonian represents a restriction, the theory still applies to many of the experimentally interesting systems [2].

Keeping in mind the above-mentioned analogy between TFG SE and stimulated emission, the desired DW representation can directly be taken over from the corresponding representation for the pump-probe spectrum (see, e.g., Refs. [1,3,30]). The result reads

$$S_{st}(t_0,\omega_0)\sim\mathrm{Tr}[W(\omega_0)G(t_0)D(\omega_L)]. \quad (19)$$

Here

$$D(\omega_L)=\int_{-\infty}^{\infty}dt'\int_{0}^{\infty}dt_1\,E_L(t')E_L(t'-t_1)e^{i\omega_Lt_1}e^{iH_et'}\times e^{-iH_et_1}V_{eg}\rho_ge^{iH_gt_1}V_{ge}e^{-iH_et'}+\text{H.c.} \quad (20)$$

is the doorway operator,

$$W(\omega_0)=\int_{-\infty}^{\infty}dt\int_{0}^{\infty}dt_3\,E_t(t+t_3)E_t(t)e^{(i\omega_0-\gamma)t_3}e^{iH_et}V_{eg}\times e^{iH_gt_3}V_{ge}e^{-iH_et_3}e^{-iH_et}+\text{H.c.} \quad (21)$$

is the window operator,

$$G(t)X=e^{-iH_et}Xe^{iH_et}\quad\forall\,X \quad (22)$$

is the excited-state propagator, V_{eg} and V_{ge} are the transition dipole moments (these are constants in the Condon approximation),

$$\rho_\alpha \equiv Z_\alpha^{-1} e^{-H_\alpha/kT} \tag{23}$$

are the equilibrium vibrational distributions in the ground ($\alpha=g$) and excited ($\alpha=e$) states, and Z_α are the corresponding partition functions.

We thus can think of the fluorescence emission as a stepwise process, which proceeds via optical creation of population in the excited state, its subsequent propagation and fluorescence emission. Evidently, the entire information about the TFG process is contained in the window operator (21). When $\gamma=0$, one recovers the standard window operator for pump-probe spectroscopy [see, e.g., Eq. (13.4a) in Ref. [1]]. In the opposite limit, $\gamma\to\infty$, the frequency resolution disappears entirely, $W_0(\omega_0)\approx 1/\gamma$, so that the TFG SE reflects the time-dependent excited-state population,

$$S_{st}(t_0,\omega_0)\sim \mathrm{Tr}[G(t_0)D(\omega_L)]=\langle \rho_e(t_0)\rangle .$$

Starting from the DW representation, we can immediately establish several general properties of the TFR spectra. If $t_0=0$, the TFG spectrum is just the trace of the product of the doorway and window wave packets. Since the doorway function represents the initial population of the electronically excited state, the corresponding TFG spectrum can be interpreted as SE from that nonequilibrium excited state. In the opposite extreme case, $t_0\to\infty$, there are two possibilities. First, if our system is coupled to a dissipative bath, then eventually

$$G(t_0\to\infty)D(\omega_L)\to\rho_e .$$

If, in addition, the time-gate function is short enough at the time scale of nuclear motion, but long enough compared with the optical coherence dephasing time, one arrives at the so-called snapshot limit for the window function [1], in which

$$W_0(\omega_0)=\int_0^\infty dt_3\, e^{(i\omega_0-\gamma)t_3} V_{eg} e^{iH_g t_3} V_{ge} e^{-iH_e t_3} + \mathrm{H.c.}, \tag{24}$$

so that

$$S_{st}(t_0\to\infty,\omega_0)\to \mathrm{Tr}[W_0(\omega_0)\rho_e].$$

This is nothing else than the relaxed fluorescence spectrum, in which γ plays the role of the inverse fluorescence lifetime. To put it differently, the TFG SE spectrum tends to a certain asymptotic spectrum, which reflects emission from the equilibrated excited-state distribution ρ_e.

If one considers nondissipative system dynamics, then the limit $G(t_0\to\infty)D(\omega_L)$ does not exist, and the TFG spectrum mirrors the oscillatory motion of the wave packet in the excited state. Generally, if the dissipation is not very strong, the processes of fluorescence and intramolecular dissipation are in competition, resulting in a time-dependent fluorescence shift and an oscillatory approach to the asymptotic relaxed fluorescence spectrum (see Sec. V). Note also that the doorway function (20) is nothing else than the asymptotic (at times much greater than the excitation-pulse duration) value of the density matrix, evaluated to the leading (second-order) contribution in the perturbation expansion. Alternatively (and more accurately), it can be computed nonperturbatively in the pump field, by including the field-matter interaction during the excitation in the system Hamiltonian [22,37]. The same applies for the evaluation of the window function.

IV. TFG SPONTANEOUS EMISSION: COMPUTATIONAL ASPECTS

Equations (19)–(21) open the way for the implementation of several approximations, which are valid provided the pulse duration is much shorter than the time scale of vibrational relaxation or much longer than the electronic dephasing time [1,3]. Here we would like to emphasize quite different aspects. Up to this moment, the precise meaning of the Hamiltonians H_g and H_e in Eq. (18) has not been specified yet. If one wishes to study the relaxation behavior of molecules, it is natural to consider a system (the chromophore) that is coupled to an environment. The vibrational Hamiltonians are written as

$$H_g=H_g^S+H_g^B+H_g^{SB}, \quad H_e=H_e^S+H_e^B+H_e^{SB}, \tag{25}$$

where the superscripts "S" and "B" denote the system and the bath, respectively. In a typical application, the system part H^S of the Hamiltonian represents the few active vibrational modes that are directly coupled to the electronic transition, while the bath represents the manifold of inactive vibrational modes of the molecule and/or the degrees of freedom of the solvent.

If the excitation and the gate pulses are short enough at the time scale of the system-bath relaxation, one can safely substitute the corresponding total Hamiltonian operators by their system parts in the doorway (20) and window (21) operators, i.e.,

$$H_g\to H_g^S, \quad H_e\to H_e^S . \tag{26}$$

This justifies the evaluation of the DW functions in terms of the eigenvalues and eigenfunctions of these system Hamiltonians,

$$H_g^S|n\rangle=E_n|n\rangle, \quad H_e^S|\alpha\rangle=E_\alpha|\alpha\rangle \tag{27}$$

(hereafter, the eigenvalues and eigenfunctions of H_g^S and H_e^S are denoted by Latin and Greek letters, respectively). The corresponding frequencies read

$$\omega_{\alpha n}=E_\alpha-E_n, \quad \omega_{\alpha\beta}=E_\alpha-E_\beta . \tag{28}$$

It is important to remark that such an eigenvalue representation is computationally feasible for system Hamiltonians containing up to three vibrational modes with electronic interstate couplings [2,38,39], so that the use of Eqs. (27) is not very restrictive. One can additionally assume that the time-gate functions and the excitation pulses are exponential and

described by equations like Eq. (3). It may seem somewhat unrealistic to model the envelopes of laser pulses by exponentials, but, at the qualitative level at least, it is justified. It has been shown that the substitution of ''actual'' Gaussian pulse envelopes by their exponential counterparts does not give rise to substantial quantitative differences in the pump-probe signals [13,25]. This approximation makes it possible to analytically perform all the time integrations in Eqs. (20) and (21), with the result:

$$S_{st}(t_0,\omega_0)\sim\sum_{\alpha,\beta,\alpha_1,\beta_1} W_{\alpha\beta}(\omega_0)G^{\alpha\beta}_{\alpha_1\beta_1}(t_0)D_{\alpha_1\beta_1}(\omega_L), \tag{29}$$

where

$$D_{\alpha\beta}(\omega_L)=\sum_n V_{\alpha n}V_{n\beta}\rho_g(n)\left\{\frac{1}{\Gamma_L-i(\omega_L-\omega_{\alpha n})}\frac{1}{\Gamma_L-i(\omega_L-\omega_{\beta n})}+\frac{1}{2\Gamma_L-i\omega_{\alpha\beta}}\frac{1}{\Gamma_L-i(\omega_L-\omega_{\beta n})}+\frac{1}{2\Gamma_L+i\omega_{\alpha\beta}}\frac{1}{\Gamma_L-i(\omega_L-\omega_{\alpha n})}\right\}+\text{c.c.}, \tag{30}$$

$$W_{\alpha\beta}(\omega_0)=\sum_n V_{\alpha n}V_{n\beta}\left\{\frac{1}{\Gamma+\gamma-i(\omega_0-\omega_{\alpha n})}\frac{1}{\Gamma+\gamma-i(\omega_0-\omega_{\beta n})}+\frac{1}{2\Gamma-i\omega_{\alpha\beta}}\frac{1}{\Gamma+\gamma-i(\omega_0-\omega_{\beta n})}+\frac{1}{2\Gamma+i\omega_{\alpha\beta}}\frac{1}{\Gamma+\gamma-i(\omega_0-\omega_{\alpha n})}\right\}+\text{c.c.} \tag{31}$$

If one wishes to develop the DW description beyond the slowly varying envelope approximation, it is possible to start from the definition (21) for the window function, but with the gate function $E_t(t;t_0)$ substituted by its generalized counterpart $\overline{E}_t(t;t_0)$ (13). One can then analytically obtain the analog of Eq. (31), but we avoid doing that here in order not to overburden the paper with technical details.

If one considers a bath-free material system, then

$$G^{\alpha\beta}_{\alpha_1\beta_1}(t_0)=e^{-i\omega_{\alpha\beta}t_0}\delta_{\alpha\alpha_1}\delta_{\beta\beta_1} \tag{32}$$

so that

$$S_{st}(t_0,\omega_0)\sim\sum_{\alpha,\beta} W_{\alpha\beta}(\omega_0)e^{-i\omega_{\alpha\beta}t_0}D_{\alpha\beta}(\omega_L). \tag{33}$$

This is nothing else than a compact form of the formula obtained by Kowalczyk *et al.* [Ref. [25], Eq. (17)] and subsequently rederived by Santoro *et al.* [Ref. [13], Eq. (11)]. The formula in Ref. [13] additionally contains contributions due to the time derivatives of the dipole moments (cf. the discussion in Sec. II). If the frequency filter is good enough ($\Gamma\gg\gamma$) and if $1/\Gamma$ is much shorter than the characteristic vibrational relaxation time and much longer than the optical coherence dephasing time, one arrives at an ideal (snapshot) TFG spectrum [31]. In that case

$$W_{\alpha\beta}(\omega_0)\approx\frac{1}{2\Gamma}\sum_n V_{\alpha n}V_{n\beta}\left\{\frac{1}{\Gamma-i(\omega_0-\omega_{\beta n})}+\frac{1}{\Gamma-i(\omega_0-\omega_{\alpha n})}\right\}+\text{c.c.} \tag{34}$$

As has been explained above [see Eqs. (12)–(14)], the ideal spectrum $S_0(t_0,\omega_0)\sim\omega_0^4$. Therefore, to find the number of photons passed through the detector, one must divide $S_0(t_0,\omega_0)$ by ω_0, which gives rise to a ω_0^3 dependence of the signal. Keeping this in mind, one immediately notes that Eq. (29) with the window function (34) recovers the result by Jean [12] and Lin *et al.* [18,19] obtained for an ideal time and frequency resolved SE spectrum. The present analysis therefore bridges the gap between the different formulations of the TFG SE signal [1,12,14,16,18,19–21], [2,5,6,13,25,26,29–31], and [3,27], and also provides the criterion of the validity of passing from ''real'' to ''bare'' SE spectra.

In order to propagate $D(\omega_L)$ for a time t_0, we can switch from the entire (system plus bath) phase space to that of the system only. This is a standard procedure in problems of this kind [1]. It is believed that, in doing so, we do not introduce significant errors into the description. One thus can regard $D(\omega_L)$ as the initial value of the reduced (system) density matrix in the excited state, which subsequently evolves according to the appropriate kinetic equation of motion. One can invoke, e.g., certain phenomenological dissipative equations [2,3,11,14], or the Redfield formalism in various approximations [2,12,27,32,33,38–41], or the semiclassical and quantum Fokker-Planck equations [22,42,43]. For instance, if one adopts the optical dephasing model, in which the electronic population and alignment possess the decay times T_1 and T_2, respectively (see papers [2,11,14] for the necessary details), Eqs. (29)–(32) are still correct if one substitutes $\gamma\rightarrow\gamma+1/T_2$ in Eq. (31), adopts a very similar equation for the doorway function (30) and multiplies Eq. (32) by $\exp(-t_0/T_1)$. If, on the other hand, the Redfield equation in the secular approximation is a correct description (it is not

infrequently so in the problems dealing with nonadiabatic coupling [38,39]), the situation simplifies considerably. In this case the density-matrix evolution $G(t)D(\omega_L)\equiv\rho(t)$ is described via

$$\frac{d}{dt}\rho_{\alpha\alpha}(t)=\sum_{\beta\neq\alpha}\Xi_{\alpha\beta}\rho_{\beta\beta}(t)-\Xi_{\alpha}\rho_{\alpha\alpha}(t),$$

$$\rho_{\alpha\alpha}(0)=D_{\alpha\alpha}(\omega_L) \tag{35}$$

$$\rho_{\alpha\beta}(t)=\exp\{-(i\omega_{\alpha\beta}+\Xi_{\alpha\beta})t\}D_{\alpha\beta}(\omega_L),\quad \alpha\neq\beta. \tag{36}$$

Here $\Xi_{\alpha\beta}$ are the damping constants due to the coupling with the bath and $\Xi_{\alpha}\equiv\Sigma_{\beta\neq\alpha}\Xi_{\beta\alpha}$. So, the TFG SE is given by the explicit formula

$$S_{st}(t_0,\omega_0)\sim\sum_{\alpha,\nu,\mu}W_{\alpha\alpha}(\omega_0)O_{\alpha\nu}e^{-\lambda_\nu t}O_{\nu\mu}D_{\mu\mu}(\omega_L)+\sum_{\alpha\neq\beta}W_{\alpha\beta}(\omega_0)\exp\{-(i\omega_{\alpha\beta}+\Xi_{\alpha\beta})t\}D_{\alpha\beta}(\omega_L). \tag{37}$$

Here $\delta_{\alpha\beta}\Xi_{\alpha}+\Xi_{\alpha\beta}\equiv\Sigma_{\nu}O_{\alpha\nu}\lambda_{\nu}O_{\nu\beta}$.

Up to now, the theory relied significantly upon the assumption that the excitation pulse and the temporal gating were well separated, so that all transient effects can be neglected. These effects manifest themselves through exponentially small contributions to the TFG SE spectra, which are proportional to the terms like $\exp(-\Gamma t_0)$ and disappear for $t_0\gg 1/\Gamma$. There exists, however, an important particular case, which allows one to explicitly incorporate the transient terms into the DW picture. Namely, let us consider the so-called impulsive excitation, when the pump pulse can be regarded as truly instantaneous on the time scale of both nuclear dynamics and electronic dephasing. By inserting the expression $E_L(t)=\delta(t)$ into Eq. (17) and making no further approximations, one also arrives at the DW formula (19), but with modified doorway $D^{imp}(\omega_L)$ and window $W^{imp}(\omega_0)$ operators. Evidently, Eq. (20) simplifies to $D^{imp}(\omega_L)=\rho_g$. On the other hand, $W^{imp}(\omega_0)$ is also given by Eq. (21) in which, however, the lower limit of integration over t changes from $-\infty$ to $-t_0$. Clearly, for $t_0\gg 1/\Gamma$ (that is tantamount to saying that the pump and gating processes are well separated) $W^{imp}(\omega_0)\rightarrow W(\omega_0)$. Moreover, following the argumentation outlined above for the standard DW operators, it is natural to invoke the eigenvalue representation (27),(28) for obtaining the explicit form of $W^{imp}(\omega_0)$. The result reads

$$W^{imp}_{\alpha\beta}(\omega_0)=W_{\alpha\beta}(\omega_0)-W^{tr}_{\alpha\beta}(\omega_0), \tag{38}$$

where $W_{\alpha\beta}(\omega_0)$ is given by Eq. (31) and

$$W^{tr}_{\alpha\beta}(\omega_0)=\sum_n V_{\alpha n}V_{n\beta}\left\{\frac{\exp\{-(2\Gamma+i\omega_{\alpha\beta})t_0\}}{2\Gamma+i\omega_{\alpha\beta}}\,\frac{1}{\Gamma+\gamma+i(\omega_0-\omega_{\beta n})}+\frac{\exp\{-[\Gamma+\gamma-i(\omega_0-\omega_{\alpha n})]t_0\}}{\Gamma+\gamma-i(\omega_0-\omega_{\alpha n})}\left[\frac{1}{\Gamma+\gamma-i(\omega_0-\omega_{\beta n})}+\frac{1}{\Gamma+\gamma+i(\omega_0-\omega_{\beta n})}\right]\right\}+\text{c.c.} \tag{39}$$

As is expected, the transient terms influence the TFG SE at times $t_0\sim 1/\Gamma$ (see also Sec. V) but vanish for $t_0\gg 1/\Gamma$. The above results show that, if one intends to extract information about the system dynamics from the TFG SE spectra, there is no intrinsic limitation to the duration of the pump pulse, since its variation just modifies the doorway function, i.e., the initial vibrational distribution in the excited state. In that sense, the δ-excitation pulse creates the most natural distribution, by merely transferring ρ_g into the excited state without distortions. On the other hand, if one wishes to monitor the SE with time and frequency resolution, the gating time should not be too small. Otherwise ($\Gamma\gg 1$), the spectral resolution is completely lost.

V. TFG SPONTANEOUS EMISSION: SPECIFIC EXAMPLES AND DISCUSSION

To illustrate the material of the preceding sections, we invoke the Condon approximation ($V_{eg}=V_{ge}=1$) and consider the standard benchmark system, consisting of displaced harmonic oscillators in the ground and excited states, which are bilinearly coupled to a harmonic bath. In this case, the third-order response functions $R_i(t_3,t_2,t_1)$ are uniquely determined by the line shape function

$$g(t)=\int_0^t dt'\int_0^{t'}dt''\,C(t'')\equiv\int_0^t dt'(t-t')C(t'), \tag{40}$$

where $C(t)=\langle e^{iH_g t}Ue^{-iH_g t}U\rho_g\rangle$ is the energy-gap CF [1] ($U\equiv H_e-H_g$).

To investigate the influence of the dissipative environment on the TFG SE, we perform explicit calculations of TFG spectra by invoking the so-called Drude model for $C(t)$ [1,20,44–47], i.e., we consider a thermal bath with exponential memory kernel. *Inter alia*, this allows us to explore the influence of non-Markovian effects on the vibrational relaxation. The conventional (Markovian) description is valid provided that the bath relaxation time is much shorter than all other relevant times of the problem. If one studies ultrafast relaxation dynamics, the Markovian assumption should be

implemented with a certain caution, since it could be an unjustified oversimplification (see, e.g., recent references [48–54]). There exist also experimental evidences that non-Markovian effects could be important, e.g., for describing vibrational relaxation in hydrogen-bonded liquids (see Ref. [34] and references therein). These effects manifest themselves through the multiexponentiality of the energy-gap CF. It is an additional advantage of the Drude model that it is not limited to weak system-bath coupling. This allows one to continuously follow the transformation of the TFG spectra from the bath free to the overdamped limit.

The Drude model leads to the following expressions for the line shape functions [46,47]

$$g(t)=g'(t)+ig''(t), \quad C(t)=C'(t)+iC''(t), \tag{41}$$

$$C'(t)=\lambda[C_1'e^{-z_1t}+C_2'e^{-z_2t}+C_3'e^{-z_3t}-\Gamma(t)], \tag{42}$$

$$C''(t)=\lambda(C_1''e^{-z_1t}+C_2''e^{-z_2t}+C_3''e^{-z_3t}). \tag{43}$$

Here λ is the Stokes shift,

$$z_1=\alpha+i\eta, \quad z_2=\alpha-i\eta, \quad z_3=\delta \tag{44}$$

are the roots of the cubic equation

$$z^3-\omega_D z^2+(1+\Lambda\omega_D)z-\omega_D=0, \tag{45}$$

and the other parameters are given by the expressions

$$C_1''=-\frac{i}{2\eta}\frac{\alpha-i\eta+\delta}{\alpha+i\eta-\delta}, \quad C_2''=\frac{i}{2\eta}\frac{\alpha+i\eta+\delta}{\alpha-i\eta-\delta}, \tag{46}$$

$$C_3''=\frac{2\alpha}{(\alpha-i\eta-\delta)(\alpha+i\eta-\delta)}, \quad C_i'=C_i''\cot(\epsilon),$$

$$\epsilon=\frac{\hbar\Omega}{2kT}, \tag{47}$$

$$\Gamma(t)=\frac{2\Lambda\omega_D^2}{\epsilon}\sum_{n=1}^{\infty}\frac{\nu_n e^{-\nu_n t}}{(z_1^2-\nu_n^2)(z_2^2-\nu_n^2)(z_3^2-\nu_n^2)},$$

$$\nu_n=\pi n/\epsilon. \tag{48}$$

Ω is the unperturbed oscillator frequency. Hereafter, we use dimensionless variables, in which time is measured in units of Ω^{-1}. Λ controls the strength of the system-bath coupling. When $\Lambda=0$, one recovers the case of free oscillators, $\Lambda \gg 1$ corresponds to the overdamped oscillator limit. ϵ [see Eq. (47)] is the ratio of zero-point energy and thermal energy of the oscillator. ω_D is responsible for the memory effects, and $1/\omega_D$ can be regarded as the bath relaxation time, so that $\omega_D \exp(-\omega_D t)$ is the memory kernel in the corresponding semiclassical generalized Langevin equation for the energy-gap coordinate (see [1,20,44–47]). When $\omega_D \to \infty$, one recovers the standard Markovian description.

To render the presentation more transparent and to visualize the dynamic and transient effects, we restrict ourselves to the case of impulsive excitation (cf. the discussion above). In that case, Eqs. (17) and (19) reduce to

$$S_{st}(t_0,\omega_0)\sim \mathrm{Re}\int_0^\infty dt\int_0^\infty dt_3\, E_t(t-t_0)E_t(t-t_3-t_0) \times\{e^{-g(t_3)^*-2i[g''(t)-g''(t-t_3)]}e^{[-\gamma+i(\omega_0-\omega_{eg})]t_3}\}. \tag{49}$$

Here $\omega_{eg}\equiv\langle H_e-H_g\rangle\equiv\omega_{eg}^0+\lambda$, and ω_{eg}^0 is the frequency of the 0-0 transition. The formula (49) allows us to calculate TFG spectra for different values of the parameters of the model and for various qualities of the time and frequency filters (see Figs. 1–4). Note that the frequency origin is chosen as ω_{eg} in these figures.

To separate the influence of the quality of temporal and spectral filtering from the dynamic effects, we start with the consideration of the TFG SE of the dissipation-free oscillators ($\Lambda=0$). We consider the case of a large Stokes shift ($\lambda=5$) and low temperature ($\varepsilon=10$). Fig. 1(a) corresponds to the case of good spectral resolution ($\gamma=0.3$) but poor temporal resolution ($\Gamma=0.2$). The TFG spectrum changes only slightly with time. It looks almost static, since the fundamental vibrational period τ_Ω (which equals 2π in our dimensionless units) is of the order of the characteristic gating time $1/\Gamma$. The spectrum exhibits a double ridge structure, which reflects the locations of the wave packet on the excited-state potential surface in the vicinity of the classical turning points. That is why the local maxima of the right (left) ridge occur at $t_0=0,2\pi,4\pi,\ldots$ ($t_0=\pi,3\pi,\ldots$). Since quantum effects are pronounced ($\epsilon=10$) and the frequency resolution is high, the spectrum possesses vibrational structure.

If one improves the temporal resolution ($\Gamma=1$), the following qualitatively new properties emerge [Fig. 1(b)]. First, the formerly static spectrum acquires pronounced dynamic features and exhibits an oscillatory behavior, which mirrors the motion of the wave packet in the excited state. Evidently, the frequency of these oscillations coincides with the free oscillator frequency $\Omega=1$. Second, the vibrational structure completely disappears, despite the fact that the frequency resolution is kept unchanged. The maxima of the TFG SE signal correspond to the classical turning points of the wave packet in the excited state as discussed above. So, in the vicinity of these points ($t_0=\pi,2\pi,3\pi,\ldots$), the wave packet rephases and becomes narrow. On the contrary, it develop the maximal speed near the potential minimum ($t_0=\pi/2,3\pi/2,5\pi/2,\ldots$) and, therefore, broadens. The signal thus monitors not only the position of the wave packet, but also the speed of the wave-packet motion. By comparing Fig. 1(b) with those from, e.g., the reviews [2,55], one sees that the overall behavior of the TFG SE signal and the stimulated-emission contribution to the integral pump-probe signal is esentially the same. In general, $S_{st}(t_0,\omega_0)$ can be regarded as a progression of instantaneous (at a particular t_0) spectra, which exhibit a time-dependent shift. Since there is no dissipation, $S_{st}(t_0,\omega_0)$ is τ_Ω periodic, but the widths and heights of the maxima of these instantaneous spectra are t_0 dependent.

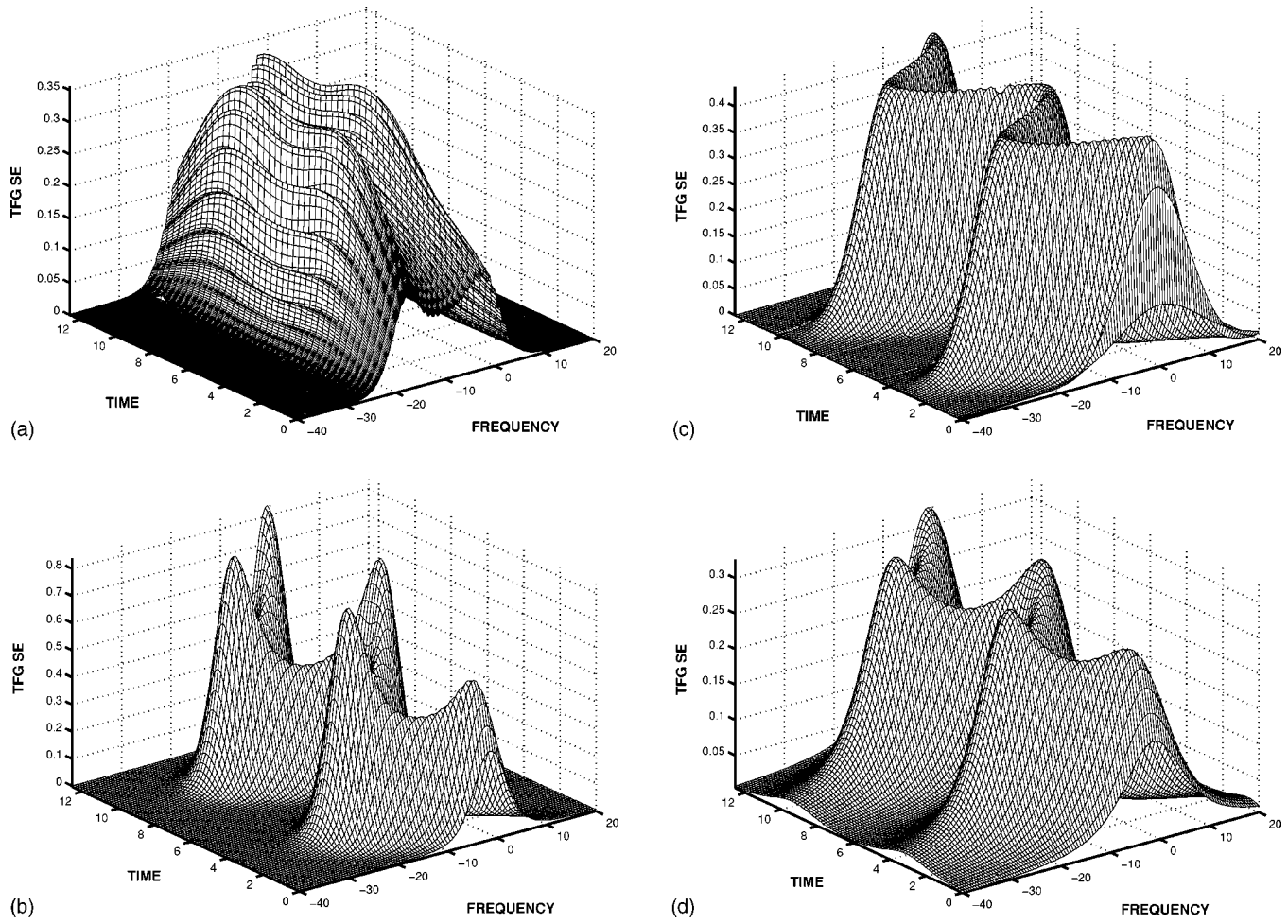

FIG. 1. Influence of temporal and spectral resolution on the SE spectrum of a bath-free ($\Lambda=0$) displaced ($\lambda=5$) harmonic oscillator in the low-temperature limit ($\epsilon=10$) with (a) $\gamma=0.3$ (good spectral resolution) and $\Gamma=0.2$ (poor time resolution); (b) $\gamma=0.3$ and $\Gamma=1$ (satisfactory time resolution); (c) $\gamma=0.3$ and $\Gamma=5$ (high time resolution); (d) $\gamma=5$ (poor frequency resolution) and $\Gamma=1$. The TFG SE intensity is given in arbitrary units. All the other parameters are dimensionless, the free oscillator frequency Ω is taken as the frequency unit and its inverse $1/\Omega$ as the time unit.

This kind of behavior should be contrasted with that depicted in Fig. 1(c), in which $S_{st}(t_0,\omega_0)$ is shown for the case of high temporal resolution ($\Gamma=5,1/\Gamma\ll\tau_\Omega$), the other parameters being unchanged. This situation corresponds, in fact, to the ideal (snapshot) TFG SE spectrum. As in the previous figure, $S_{st}(t_0,\omega_0)$ is τ_Ω periodic, but the widths and heights of the maxima of the instantaneous spectra are almost t_0 independent. The explanation of these qualitative changes is provided by Eqs. (31)–(34). To calculate the ideal TFG spectrum for a dissipation-free system, one may use Eqs. (33) and (34). The inspection of these formulas reveals that $S_0(t_0,\omega_0)$ consists of a sum of Lorentzians that are multiplied by time-dependent factors $e^{-i\omega_{\alpha\beta}t_0}$. Note that these factors are determined by the transition frequencies in the excited state. For a particular t_0, these factors just single out the maximal contributions to $S_0(t_0,\omega_0)$, corresponding to $\omega_{\alpha\beta}t_0=2\pi n$ $(n=0,1,2,\ldots)$. On the other hand, the widths and heights of the Lorentzians are time independent and specified by the $e\rightarrow g$ transition frequencies $\omega_{\alpha n}$. If one considers the TFG SE beyond the snapshot limit, one should employ the more general Eq. (31) for the window function. It also can approximately be regarded as a sum of certain ''spectral functions,'' multiplied by the same time-dependent factors $e^{-i\omega_{\alpha\beta}t_0}$. In contrast to the snapshot case, the ''spectral functions'' are the products of two Lorentzians, which are both $\omega_{\alpha n}$ and $\omega_{\alpha\beta}$ dependent. So, in general, the excited-state frequencies $\omega_{\alpha\beta}$ affect the widths and maxima of $S_{st}(t_0,\omega_0)$ and, therefore, make these t_0 dependent. When Γ is further increased, the spectral features of $S_{st}(t_0,\omega_0)$ are smeared out. In principle, any frequency resolution disappears in the limit $\Gamma\gg1$, in which one merely measures the time-dependent population in the excited state, since $S_{st}(t_0,\omega_0)\rightarrow \mathrm{Tr}[G(t_0)D(\omega_L)]$. Similarly, if the spectral resolution decreases ($\gamma=5$), the TFG SE broadens and tends to become more featureless [Fig. 1(d)]. In this sense, poor spectral resolution ($\gamma\gg1$) is equivalent to high temporal resolution ($\Gamma\gg1$).

By inspecting Figs. 1(a)–1(d), as well as the subsequent Figs. 2 and 3, one clearly observes the signature of the transient effects. These manifest themselves through the increase of the area under the instantaneous spectra $S_{st}(t_0,\omega_0)$ at short times. In other words, the TFG SE spectra ''flare up''

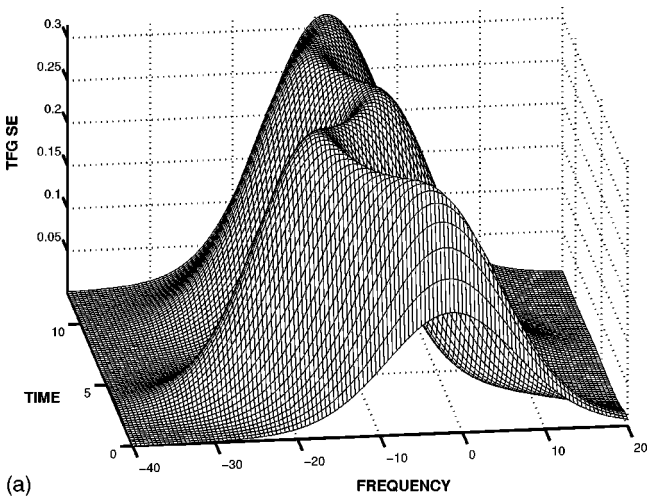

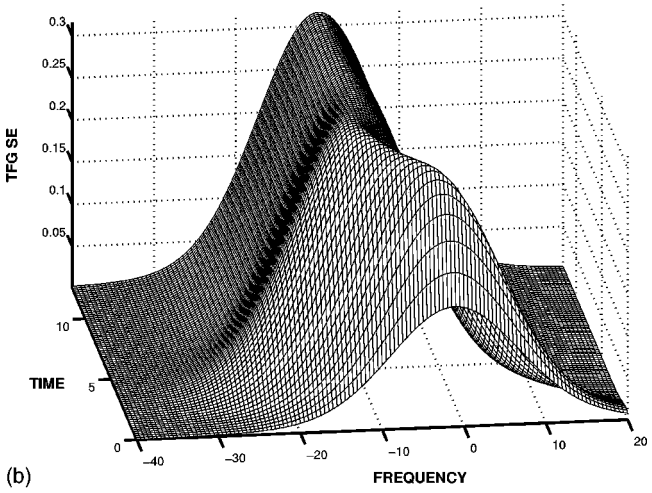

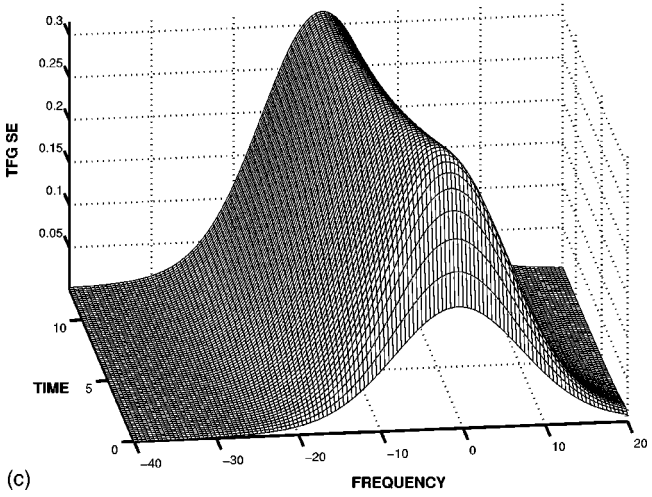

FIG. 2. Manifestation of the dissipation strength in the TFG SE spectrum in the case of satisfactory time and frequency resolution ($\gamma=\Gamma=1$) for a classical ($\epsilon=0.1$) displaced ($\lambda=5$) harmonic oscillator coupled to a Markovian bath. (a) $\Lambda=0.3$ (underdamped oscillator); (b) $\Lambda=1$ (moderately damped oscillator); (c) $\Lambda=5$ (overdamped oscillator).

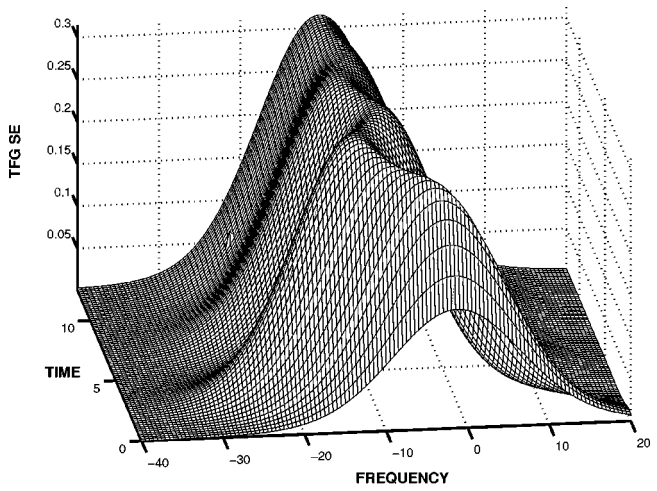

FIG. 3. TFG SE spectrum in the case of satisfactory time and frequency resolution ($\gamma=\Gamma=1$) for a classical ($\epsilon=0.1$) displaced ($\lambda=5$) harmonic oscillator moderately ($\Lambda=1$) coupled to a highly non-Markovian bath ($\omega_D=1$).

on a time scale of $1/\Gamma$. The origin of this phenomenon has been discussed at the end of Sec. IV [see Eqs. (38) and (39)]. Here we present the corresponding quantitative estimates. Integrating Eq. (49) over ω_0 one finds that, irrespective of the particular form of $g(t)$,

$$\int_{-\infty}^{\infty} d\omega_0\, S_{st}(t_0,\omega_0) \sim \int_{-t_0}^{\infty} dt\, E_t^2(t) = \frac{1}{2\Gamma}\begin{cases} \sqrt{\frac{\pi}{2}}[1+\Phi(t_0)] & \text{for Eq. (2)} \\ 2-e^{-2\Gamma t_0} & \text{for Eq. (3)}, \end{cases} \tag{50}$$

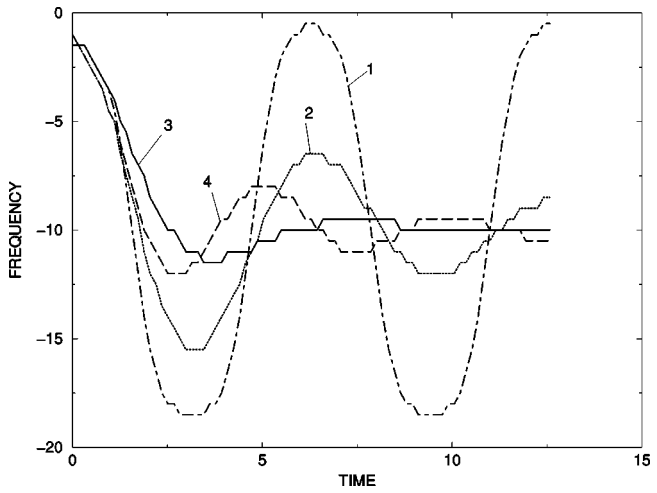

FIG. 4. Time evolution of the maxima of instantaneous TFG SE spectra in the case of satisfactory time and frequency resolution ($\gamma=\Gamma=1$) for a classical displaced harmonic oscillator ($\epsilon=0.1, \lambda=5$) coupled to different baths. (1) $\Lambda=0$ (free oscillator); (2) $\Lambda=0.3$ (underdamped Markovian oscillator); (3) $\Lambda=1$ (moderately damped Markovian oscillator); (4) $\Lambda=1$, $\omega_D=1$ (moderately damped non-Markovian oscillator).

where Φ is the error function. This result shows that the initial ($t_0=0$) area under the TFG SE spectrum is smaller by a factor of two than the asymptotic ($t_0\to\infty$) area. Evidently, the better the temporal resolution, the less visible are the transient effects.

Having established the influence of the quality of the TFG procedure on the SE, we turn to the investigation of the manifestation of dissipative effects in the TFG SE. To this end, we consider different kinds of dissipation mechanisms. The standard Markovian bath is studied first. Figures 2(a)–2(c) show the TFG SE spectra obtained for increasing strength of the system-bath coupling. A large Stokes shift ($\lambda=5$) and high temperature ($\varepsilon=0.1$) are assumed, as well as good time and frequency resolution ($\gamma=\Gamma=1$). The evolution of the TFG SE spectra reflects the strength of system-bath coupling, as expected. The initial spectrum, $S_{st}(0,\omega_0)$, eventually develops into the asymptotic one, $S_{st}(\infty,\omega_0)$, which exhibits the Stokes shift of 2λ. When the damping effects are not strong, the system dynamics is underdamped and the signal exhibits weakly damped oscillations [Fig. 2(a)]. When the dissipation strength is further increased, the wave-packet oscillations are rapidly damped [Fig. 2(b)]. In the overdamped limit, $S_{st}(0,\omega_0)$ tends to $S_{st}(\infty,\omega_0)$ monotonously [Fig. 2(c)].

To get a better understanding of the TFG SE of the overdamped oscillator, it is useful to calculate the spectrum analytically. Moreover, one can surmount the restriction of impulsive excitation and assume that the pump and gate pulses have a Gaussian shape [Eq. (2)]. The spectral filter is assumed to be "ideal" ($\gamma=0$). To arrive at the desired result, one can start either from the general Eq. (17), or from the DW description (19)–(21). Let us assume, in addition, that the oscillator motion is much slower than the optical dephasing time. This allows us to neglect the system dynamics during t_3 and t_1, when the system is in the coherence state. We can thus retain only the leading contributions to the g functions, up to quadratic terms in t_3 and t_1. The corresponding expression has been derived and discussed in Refs. [1,44,56,57] for the sequential pump-probe spectrum, but we can further generalize it by invoking the modified gate function (14). The result reads

$$S_t(t_0,\omega_0)=\frac{2\pi(3A^2+6AB^2+B^4)}{\sqrt{(\Delta^2+\Gamma_L^2)\alpha^2(t_0)}}\times\exp\left\{-\frac{\overline{\omega_L}^2}{2(\Delta^2+\Gamma_L^2)}\right\}\times\exp\left\{-\frac{[\overline{\omega}_0-\overline{\omega}(t_0)]^2}{2\alpha^2(t_0)}\right\}. \tag{51}$$

Here

$$\overline{\omega}_L=\omega_L-\omega_{eg},\quad \overline{\omega}_0=\omega_0-\omega_{eg},$$

$$\tilde{\omega}=\overline{\omega}_L\frac{\Delta^2}{\Delta^2+\Gamma_L^2},\quad \Delta^2\equiv 2\lambda kT/\hbar, \tag{52}$$

$$\overline{\omega}(t)=-2\lambda+e^{-\Lambda t}(\tilde{\omega}+2\lambda), \tag{53}$$

$$\alpha^2(t)=\Delta^2\left[1-\frac{\Delta^2}{\Delta^2+\Gamma_L^2}e^{-2\Lambda t}\right]+\Gamma^2, \tag{54}$$

$$A=\frac{\Gamma^2\Delta^2(1-e^{-2\Lambda t})}{\Gamma^2+\Delta^2(1-e^{-2\Lambda t})},$$

$$B=\frac{[\overline{\omega}(t)+\omega_{eg}]\Gamma^2+\omega_0\Delta^2(1-e^{-2\Lambda t})}{\Gamma^2+\Delta^2(1-e^{-2\Lambda t})}. \tag{55}$$

Equation (53) allows us to visualize the origin of the time-dependent Stokes shift, which is seen to reflect the relaxation of the system towards its equilibrium in the excited state. One should also note the factor $3A^2+6AB^2+B^4$, which ensures a correct description beyond the slowly varying envelope approximation (see the pertinent discussion in Sec. II). Evidently, when ω_{eg} exceeds substantially all relevant frequencies of the problem, then $\omega_0\sim\omega_{eg}$, so that $3A^2+6AB^2+B^4\approx B^4$, where

$$B\approx\frac{\omega_{eg}\Gamma^2+\omega_0\Delta^2(1-e^{-2\Lambda t})}{\Gamma^2+\Delta^2(1-e^{-2\Lambda t})}.$$

Therefore, $B\approx\omega_0$, and the standard approximation (9) is justified. When the temporal resolution is high compared to the time scale of the inhomogeneous broadening ($\Gamma\gg\Delta$), the additional term also reduces to a constant factor. If this is not the case, the additional contribution depends in a complicated manner on t_0,ω_0 and also on the parameters determining the excitation, the system dynamics and temporal gating. It is important that Eq. (51) allows one to determine the influence of the duration of the excitation pulse on the TFG SE signal (see also, Refs. [1,3,44,56,57]). When the pulse is short ($\Gamma_L\gg 1$), the spectral width $\alpha^2(t)\approx\Delta^2+\Gamma^2$ is time independent, so that the TFG SE spectrum experiences no time-dependent broadening. In the opposite case ($\Gamma_L\ll 1$), $\alpha^2(0)<\alpha^2(\infty)$, so that the spectrum broadens. To put it differently, the finiteness of the pump duration results in a time-dependent broadening of $S_t(t_0,\omega_0)$, which is governed by the parameter $\alpha^2(t)$. When the gate pulse is truly instantaneous ($\Gamma\gg 1$), then $\alpha^2(t)\to\infty$ and the TFG spectrum loses any frequency resolution. This is an additional confirmation of the fact that an ideal time gate should be a δ function on the time scale of the system relaxation, but a constant on the time scale of the optical coherence dephasing.

Now we turn to the study of the impact of memory effects on the TFG spectra. To this end, let us compare Fig. 2(b) and Fig. 3, in which $S_{st}(t_0,\omega_0)$ is presented for the Markovian ($\omega_D\to\infty$) and the non-Markovian ($\omega_D=1$) oscillator, respectively, in the case of moderate coupling with the bath ($\Lambda=1$). In both situations, $S_{st}(t_0,\omega_0)$ eventually arrives at the relaxed spectrum. However, the manner in which this asymptotic spectrum is approached is very different in the Markovian and non-Markovian cases, respectively. Indeed, after the elapse of a characteristic time of the order of $1/\Lambda$ (this time scale is determined by the strength of the system-

bath coupling), the ''centers of gravity'' of both Markovian and non-Markovian TFG spectra exhibit the same Stokes shift. In the Markovian case, the subsequent relaxation of the spectrum occurs more or less monotonically [Fig. 2(b)]. When memory effects come into play, the TFG SE signal tends to the relaxed spectrum nonmonotonically, its ''center of gravity'' exhibiting pronounced oscillatory behavior (Fig. 3). The TFG SE spectrum of the underdamped Markovian oscillator [Fig. 2(a)] looks qualitatively similar to the spectrum of the moderately damped non-Markovian oscillator (Fig. 3). The question therefore arises: is it possible to distinguish between these two situations?

It is Eq. (45) that allows one to answer this question. Evidently, the two roots z_1 and z_2 of this equation can be either real and positive [if η in Eq. (44) is imaginary], or complex conjugate to each other, with a positive real part (if η is real). The third root z_3 is always real and positive. Clearly, if all roots are positive, the system relaxes to its equilibrium distribution monotonically. This is so, e.g., in the overdamped Markovian case [Fig. 2(c)]. If Eq. (45) possesses two complex conjugated roots, it is the magnitude of η which determines the fundamental oscillation frequency of the problem. It is possible to derive an analytical expression for η, but it turns out to be cumbersome and difficult to analyze. For our purpose it is sufficient to realize that, in the Markovian limit ($\omega_D \to \infty$), the cubic equation (45) reduces to a quadratic equation, yielding $\eta = \sqrt{1-\Lambda^2/4}$ (recall that the unperturbed oscillator frequency is $\Omega = 1$). On the other hand, one gets a simple solution of Eq. (45) in the overdamped ($\Lambda \gg 1$), but strongly non-Markovian ($\omega_D \sim 1$) case: $\eta \approx \sqrt{\Lambda \omega_D}$. So, one arrives at the remarkable conclusion that in the Markovian limit the oscillation frequency η cannot exceed the free oscillator frequency $\Omega = 1$, while in the non-Markovian case it can. To put it differently, the period of the wave-packet oscillations in the Markovian limit can be 2π (free oscillator) or larger (underdamped oscillator), while in the non-Markovian case that period can be less than 2π. This observation allows one to distinguish between the damped non-Markovian and underdamped Markovian oscillators, if one knows the unperturbed oscillator frequency Ω.

These qualitative considerations are confirmed by numerical computations of $S_{st}(t_0, \omega_0)$, as depicted in Fig. 4. It shows the positions of the maxima of instantaneous TFG SE spectra (with $\gamma = \Gamma = 1$) as a function of the gating time t_0 for a displaced oscillator ($\lambda = 5$) in the high-temperature limit ($\varepsilon = 0.1$). It is seen that the TFG spectra exhibit 6.3 (free oscillator), 4.8 (non-Markovian damped oscillator), and 6.4 (underdamped Markovian oscillator) periodic oscillations. The message is that the TFG SE signal of a system coupled to a non-Markovian bath can exhibit pronounced oscillations with a period that is less than that of the bath-free system. This qualitative effect can be helpful for the estimation of the importance of memory effects in dissipative systems.

Summarizing, the interpretation of the TFG SE spectra can provide us with a certain knowledge not only on the strength of the system-bath coupling, but also on the bath correlation function.

VI. CONCLUSIONS

The ultimate goal of the present work is the development of a computationally oriented framework for the description of TFG SE of nontrivial systems, that is, multimode systems with strong electronic interstate couplings, which interact with a thermal bath. The specific tasks are as follows: (i) to develop a universal, eigenstate free, description of the TFG SE, (ii) to clarify the influence of the spectral filtering and temporal gating on the TFG SE spectra, and (iii) to connect the measured TFG SE spectra with the time evolution of the corresponding material systems.

The material-system dynamics has been shown to enter the description in terms of the two-time CF of the second derivatives of the transition dipole moment [Eqs. (1) and (8)]. In the evaluation of the CF, retardation effects due to the finiteness of the speed of light should be taken into account. The CF, convoluted appropriately with the corresponding time-gate and filter functions, yields the experimentally measured TFG SE spectra. The convolution requires three consecutive time integrations to be performed. It has been demonstrated that, by taking the standard Fabry-Perot-like frequency-filter function (4), one of these integrations can be performed analytically [Eq. (15)], irrespective of a particular form of the CF (8) and the time-gate function. The validity of the commonly employed approximation (9) has been discussed and generalized expressions have been derived for the TFG SE in terms of Wigner spectrograms beyond this approximation. The retardation effects are demonstrated to give rise to a redefinition (back shift) of the time origin of the TFG SE spectrum.

We have further developed the DW picture of the TFG SE, under the assumption that the excitation and gating processes are well temporally separated. This casts the description of the TFG SE into an intuitively appealing form in terms of wave-packet dynamics in the excited state. This method requires the doorway and window operators to be calculated only once, so that subsequent propagation of the doorway operator over a time interval t_0 and its averaging together with the window operator according to Eq. (19) yield the TFG SE spectrum $S_{st}(t_0, \omega_0)$. It has been shown that the TFG SE is equivalent to the stimulated-emission contribution to the integral pump-probe spectrum. In this case the time-gate function plays the role of the envelope of the probe pulse, and the spectral filter function determines its carrier frequency. The only subtle difference stems from the imperfection of the spectral filter ($\gamma \neq 0$), but this is negligibly small for good filters.

It should be noted, however, that the equivalence between the TFG SE signal and stimulated-emission contribution to the sequential integral pump-probe signal holds only in the leading (second) order in the pump and probe pulses. In this case also the ''bare'' TFG SE spectrum coincides with the stimulated-emission contribution to the dispersed pump-probe spectrum [14,15]. It is of importance that both stimulated emission (from the electronically excited state) and stimulated Raman (from the ground state) processes contribute to the overall pump-probe signal, even in the case of sequential, nonoverlapping pump and probe pulses. On the

other hand, if the excitation and gate pulses do not overlap, the SE consists solely of the fluorescence (excited state) component. As a consequence, one cannot experimentally separate the ground and excited state contribution to the pump-probe signal. The SE signal from the excited state is, however, background free. So, in general, the TFG SE is not simply related to the pump-probe signal.

If the DW operators are expanded over the complete set of eigenfunctions of the bath-free Hamiltonian and if one assumes the exponential time-gate function (3), the DW functions can be evaluated analytically beyond the snapshot limit. The theory developed in the present work (i) allows one to establish some model-independent properties of TFG spectra, (ii) bridges the gap between the different kinds of descriptions introduced previously, (iii) helps in determining their limitations, and (iv) clarifies interconnections between ''real'' and ''bare'' spectra.

The standard displaced oscillator model bilinearly coupled to a harmonic bath has been adopted to illustrate the time-frequency evolution of the SE spectra for different regimes of dissipation. The TFG SE spectra have been found to be quite sensitive not only to the overall strength of the system-bath coupling, but also to finer features, such as memory effects. The influence of the quality of the spectral and temporal filtering on the measured TFG SE spectra also has been studied in some detail.

One of the main findings of the present work is that the specific features of the wave-packet dynamics in the excited state survive the TFG mapping procedure, and manifest themselves in the SE spectra. Recent TFG SE measurements [8–10] have confirmed the persistence of pronounced vibrational coherence effects in the obtained spectra. This underlines that the TFG SE clearly reflects the wave-packet dynamics in the excited state, provided a good compromise is found between temporal and spectral resolution. The information about the material dynamics can be extracted from the TFG SE spectra by the appropriate theoretical analysis.

ACKNOWLEDGMENTS

This work has been supported by the Deutsche Forschungsgemeinschaft through SFB 377. M.F.G. acknowledges financial support through a visitor grant.

APPENDIX

Following Mukamel and co-workers [29–33], we adopt the Wigner spectrograms for the description of the TFG SE. Let us introduce the new variables

$$\bar{t}=(t'+t'')/2, \quad s=t'-t'' \tag{A1}$$

and the bare TFG spectral function

$$S_0(\bar{t},\omega)=\int_{-\infty}^{\infty} ds\, e^{is\omega}\langle P(\bar{t}+s/2)P(\bar{t}-s/2)\rangle. \tag{A2}$$

After the insertion of Eq. (A2) into Eq. (12) one arrives at Eq. (10) in which

$$S_t(t_0,\omega_1)=\int_{-\infty}^{\infty} d\bar{t}\, d\omega\, \bar{W}(\bar{t},\omega_1-\omega,t_0)S_0(\bar{t},\omega), \tag{A3}$$

with

$$\bar{W}(\bar{t},\omega,t_0)\equiv\left(\frac{1}{4}\partial_t^2+\omega^2\right)W(\bar{t},\omega,t_0), \tag{A4}$$

$$W(\bar{t},\omega,t_0)=\int_{-\infty}^{\infty} ds\, e^{is\omega}E_t(\bar{t}+s/2;t_0)E_t^*(\bar{t}-s/2;t_0). \tag{A5}$$

One sees that the explicit inclusion of the time derivatives of the transition dipole moments results in an additional contribution to the transformation function $\bar{W}$, which is given by the term in parentheses in Eq. (A4). By using, e.g., the Gaussian gating function (2), one can evaluate $\bar{W}$ analytically,

$$W(\bar{t},\omega,t_0)=\frac{\sqrt{2\pi}}{\Gamma}\exp\left(-\frac{\omega^2}{2\Gamma^2}-2\Gamma^2(\bar{t}-t_0)^2\right), \tag{A6}$$

$$\bar{W}(\bar{t},\omega,t_0)\equiv\{[\Gamma^2(4\Gamma^2(\bar{t}-t_0)^2-1)+\omega^2]^2 -2\Gamma^4(8\Gamma^2(\bar{t}-t_0)^2-1)\}W(\bar{t},\omega,t_0). \tag{A7}$$

If the material system under study possesses a narrow spectrum in the vicinity of the frequency ω_{eg} of the electron transition, and if $\Gamma\gg\gamma$ (a good filter), then $\bar{W}\approx\omega_0^4 W$. Otherwise, one should use the more general expression (A4).

It is important that for the standard TFG functions (2)–(4) the transformation function $\bar{W}$ simplifies to $\bar{W}(\bar{t}-t_0,\omega)$. So, the bare TFG spectrum $S(t_0,\omega_0)$ and the ideal frequency filter spectrum $S_t(t_0,\omega_1)$ can be extracted from Eqs. (10) and (A3) by performing the appropriate inverse Fourier transforms. This opens the way for getting direct information about the material system from measured TFG spectra (see also papers [5–7,26]). The procedure requires, of course, the TFG SE spectra to be available with a considerable accuracy, both with respect to time and frequency.

[1] S. Mukamel, *Principles of Nonlinear Optical Spectroscopy* (Oxford University Press, New York, 1995).
[2] W. Domcke and G. Stock, Adv. Chem. Phys. **100**, 1 (1997).
[3] L. W. Ungar and J. A. Cina, Adv. Chem. Phys. **100**, 171 (1997).
[4] T. J. Dunn, J. N. Sweetser, I. A. Walmsley, and C. Radzewicz, Phys. Rev. Lett. **70**, 3388 (1993).
[5] T. J. Dunn, I. A. Walmsley, and S. Mukamel, Phys. Rev. Lett. **74**, 884 (1995).
[6] L. J. Waxer, I. A. Walmsley, and W. Vogel, Phys. Rev. A **56**,

R2491 (1997).
[7] I. A. Walmsley and L. J. Waxer, J. Phys. B **31**, 1825 (1998).
[8] I. V. Rubtsov and K. Yoshihara, J. Phys. Chem. A **103**, 10 202 (1999).
[9] I. V. Rubtsov, H. Shirota, and K. Yoshihara, J. Phys. Chem. A **103**, 1801 (1999).
[10] I. V. Rubtsov and K. Yoshihara, in *Femtochemistry*, edited by DeSchryver *et al.* (Wiley, New York, 2001).
[11] G. Stock and W. Domcke, J. Chem. Phys. **93**, 5496 (1990).
[12] J. M. Jean, J. Chem. Phys. **101**, 10 464 (1994).
[13] F. Santoro, C. Petrongolo, and A. Lami, J. Chem. Phys. **113**, 4073 (2000).
[14] S. Hahn and G. Stock, J. Phys. Chem. A **105**, 2626 (2001).
[15] S. Hahn and G. Stock, Chem. Phys. **259**, 297 (2000).
[16] M. Hayashi *et al.*, J. Phys. Chem. A **102**, 4256 (1998).
[17] R. Chang *et al.*, J. Chem. Phys. **115**, 4939 (2001).
[18] H. Lin, B. Fain, N. Hamer, and C. Y. Yeh, Chem. Phys. Lett. **162**, 73 (1989).
[19] S. H. Lin, B. Fain, and C. Y. Yeh, Phys. Rev. A **41**, 2718 (1990).
[20] Y. Zhao and R. S. Knox, J. Phys. Chem. A **104**, 7751 (2000).
[21] J. Lu, F. Shao, K. Fan, and S. Du, J. Chem. Phys. **114**, 3373 (2001).
[22] F. Shuang, C. Yang, and Y. Yan, J. Chem. Phys. **114**, 3868 (2001).
[23] J. H. Eberly and K. Wodkiewicz, J. Opt. Soc. Am. **67**, 1253 (1977).
[24] V. Wong and I. A. Walmsley, J. Opt. Soc. Am. B **12**, 1491 (1995).
[25] P. Kowalczyk, C. Radzewicz, J. Mostowski, and I. A. Walmsley, Phys. Rev. A **42**, 5622 (1990).
[26] A. Zucchetti, W. Vogel, D.-G. Welsch, and I. A. Walmsley, Phys. Rev. A **60**, 2716 (1999).
[27] L. W. Ungar and J. A. Cina, J. Phys. Chem. A **102**, 7382 (1998).
[28] A. Matro and J. A. Cina, J. Phys. Chem. **99**, 2568 (1995).
[29] S. Mukamel, C. Ciordas-Ciurdariu, and V. Khidekel, IEEE J. Quantum Electron. **32**, 1278 (1996).
[30] S. Mukamel, C. Ciordas-Ciurdariu, and V. Khidekel, Adv. Chem. Phys. **101**, 345 (1997).
[31] S. Mukamel, J. Chem. Phys. **107**, 4165 (1997).
[32] V. Chernyak, T. Minami, and S. Mukamel, J. Chem. Phys. **112**, 7953 (2000).
[33] J. C. Kirkwood, C. Scheurer, V. Chernyak, and S. Mukamel, J. Chem. Phys. **114**, 2419 (2001).
[34] P. Hamm, M. Lim, and R. M. Hochstrasser, Phys. Rev. Lett. **81**, 5326 (1988).
[35] G. S. Agrawal, *Quantum Statistical Theories of Spontaneous Emission and Their Relation to Other Approaches*, Springer Tracts in Modern Physics, Vol. 70 (Springer-Verlag, Berlin, 1984).
[36] F. Bloch and A. Siegert, Phys. Rev. **57**, 522 (1940).
[37] B. Wolfseder, L. Seidner, G. Stock, and W. Domcke, Chem. Phys. **217**, 275 (1997).
[38] A. Kühl and W. Domcke, Chem. Phys. **259**, 227 (2000).
[39] D. Egorova, A. Kühl, and W. Domcke, Chem. Phys. **268**, 105 (2001).
[40] U. Kleinekathöfer, I. Kondov, and M. Schreiber, Chem. Phys. **268**, 121 (2001).
[41] I. Kondov, U. Kleinekathöfer, and M. Schreiber, Chem. Phys. **114**, 1497 (2001).
[42] Y. Tanimura and S. Mukamel, J. Chem. Phys. **101**, 3049 (1994).
[43] Y. Tanimura and S. Mukamel, Chem. Phys. **107**, 1779 (1997).
[44] Yi Yan and S. Mukamel, J. Chem. Phys. **89**, 5160 (1988).
[45] U. Weiss, *Quantum Dissipative Systems* (World Scientific, Singapore, 1993).
[46] Y. Gu, A. Widom, and P. M. Champion, J. Chem. Phys. **100**, 2547 (1994).
[47] R. Karrlein and H. Grabert, Phys. Rev. E **55**, 153 (1997).
[48] J. Cao, J. Chem. Phys. **107**, 3204 (1997).
[49] Y. Yan, Phys. Rev. A **58**, 2721 (1998).
[50] C. Meier and D. J. Tannor, J. Chem. Phys. **111**, 3365 (1999).
[51] O. Kuhn, Y. Zhao, F. Shuang, and Y. Yan, J. Chem. Phys. **112**, 6104 (2000).
[52] Y. Yan *et al.*, J. Chem. Phys. **113**, 2068 (2000).
[53] T. Mancal and V. May, J. Chem. Phys. **114**, 1510 (2001).
[54] D. Kilin and M. Schreiber, J. Lumin. **92**, 13 (2001).
[55] W. T. Pollard and R. A. Mathies, Annu. Rev. Phys. Chem. **43**, 497 (1992).
[56] R. F. Loring, Yi Yan, and S. Mukamel, J. Chem. Phys. **87**, 5840 (1987).
[57] Y. Georgievskii, C. Hsu, and R. A. Marcus, J. Chem. Phys. **108**, 7356 (1998).